Research Paper
J. Astron. Space Sci. 40(4), 259-266 (2023)
https://doi.org/10.5140/JASS.2023.40.4.259

JASS Journal of Astronomy and Space Sciences

Search for Dark Photon in $e^+e^- \rightarrow A'A'$ Using Future Collider Experiments

Kihong Park[1,2], Kyungho Kim[2], Alexei Sytov[2,3], Kihyeon Cho[1,2†]
[1]University of Science and Technology, Daejeon 34113, Korea
[2]Korea Institute of Science and Technology Information, Daejeon 34141, Korea
[3]INFN Ferrara Division, Ferrara 44122, Italy

The Standard Model (SM) does not provide an information for 26% of dark matter of the universe. In the dark sector, dark matter is supposed to be linked with the hypothetical particles called dark photons that have similar role to photons in electromagnetic interaction in the SM. Besides astronomical observation, there are studies to find dark matter candidates using accelerators. In this paper, we searched for dark photons using future electron-positron colliders, including Circular Electron Positron Collider (CEPC)/CEPC, Future Circular Collider (FCC-ee)/Innovative Detector for Electron-positron Accelerator (IDEA), and International Linear Collider (ILC)/International Large Detector (ILD). Using the parameterized response of the detector simulation of Delphes, we studied the sensitivity of a double dark photon mode at each accelerator/detector. The signal mode is double dark photon decay channel, $e^+e^- \rightarrow A'A'$, where A' (dark photon with spin 1) decaying into a muon pair. We used MadGraph5 to generate Monte Carlo (MC) events by means of a Simplified Model. We found the dark photon mass at which the cross-sections were the highest for each accelerator to obtain the maximum number of events. In this paper we show the expected number of dark photon signal events and the detector efficiency of each accelerator. The results of this study can facilitate in the dark photon search by future electron-positron accelerators.

Keywords: astroparticle physics, dark matter, dark photon, accelerator, MadGraph5, Delphes

1. INTRODUCTION

1.1 Dark Matter Search

Astronomical studies have shown that the materials originated from the Standard Model (SM) accounts for only 4% of the components of the universe (Cho 2016; Yeo & Cho 2018). Though the SM of particle physics agrees well with experimental results, the SM does not provide an information for dark matter, which is the dominant matter component (26%) of the universe (Cho 2016; Yeo & Cho 2018). Because dark matter only interacts gravitationally with SM particles, it is difficult to detect it directly. Dark matter is known to play an important role in the evolution of the universe in constructing cosmic structures including stars, galaxies, and galaxy clusters. Furthermore, the presence of dark matter suggests the existence of the "beyond the SM" (BSM). Therefore, identifying dark matter is an important issue in modern particle physics and cosmology.

Dark matter has not been directly detected to date because its interaction with ordinary matter is very weak. Nevertheless, three types of experimental methods have been actively conducted to search for dark matter (Cho 2017; Yeo & Cho 2018). One is a direct search method used to study the signals generated by dark matter colliding with the SM particles. Another experiment is an indirect search method that observes excess gamma rays produced by the pair annihilation of dark matter in the center of the galaxy, where abundant dark matter is distributed. Finally, there is an accelerator search method that uses accelerators to study

Received 17 OCT 2023 **Revised** 01 NOV 2023 **Accepted** 19 NOV 2023
[†]**Corresponding Author**
Tel: +82-42-869-0722, E-mail: cho@kisti.re.kr
ORCID: https://orcid.org/0000-0003-1705-7399

the signals of dark matter or dark photons produced from the SM particles (Ilten et al. 2016; Aaij et al. 2018; He et al. 2018; Hearty 2022; San et al. 2022).

In this paper, we studied dark photons. Dark photons are hypothetical particles that have similar role to photons in electromagnetic interaction but have been proposed as force carriers with a potential link to dark matter (Park et al. 2021a). We have done simulation studies with a parametrized response of the detector simulation of Delphes. We presented the expected number of signal events in each experiment with the detector efficiency. We studied double dark photon decay modes using future electron-positron accelerators such as Circular Electron Positron Collider (CEPC)/CEPC, Future Circular Collider (FCC-ee)/Innovative Detector for Electron-positron Accelerator (IDEA), and International Linear Collider (ILC)/International Large Detector (ILD).

1.2 Dark Matter Search Using Electron-Positron Colliders

There are two types of accelerator-based experiments. One is based on the hadron accelerator, including the Large Hadron Collider (LHC), which exploits a proton-proton collision. The other is the lepton accelerator which uses an electron-positron collision. Fig. 1 compares the Feynman diagram of the Simplified Model for a hadron accelerator and a lepton accelerator. These two accelerators play a complementary role in the exploration of dark matter. However, electron-positron accelerator provides several favorable research environments (Yeo & Cho 2018). It has the advantage of exploring light dark matter, which has a mass range of a few MeV–GeV. In addition, it provides clean signal events and low background events compared with the hadron accelerator. As future electron-positron accelerators, there are CEPC, FCC-ee, and ILC. We study for dark sector using these electron-positron colliders. Table 1 shows parameters of electron-positron accelerators with detectors (Particle Data Group et al. 2020).

2. THEORY

2.1 Dark Photon Modes

Because the SM cannot account for dark matter, theoretical physicists assume that there is a dark sector containing dark matter (Shuve & Yavin 2014). We also assume that there are mediator particles between the SM and dark sector. In this paper, we consider a dark photon as a mediator particle. According to theory (Shuve & Yavin 2014), dark photons can only couple to muons. Based on this theory, we studied a double dark photon mode with future electron-positron accelerators. The signal mode is $e^+e^- \rightarrow A'A'$ where each A' (dark photon with spin 1) decays into dimuon. That is, the final state particles are four muons for the decay mode of $e^+e^- \rightarrow A'A'$. Fig. 2 shows a dominant Feynman diagram of the double dark photon mode. $g^{V}_{l_{11}}$ is the coupling between the electron and dark photon. $g^{V}_{l_{22}}$ is the coupling between the muon and dark photon. Table 2 summarizes the coupling constants.

2.2 Simplified Model

To study dark matter, we used Simplified Model (Morgante 2018). This model is minimally extended from the SM. It includes not only SM particles but also dark matter and mediators, including dark photons. The Simplified Model is located between the ultraviolet and the effective field theory models (Morgante 2018). Originally, this model was used for hadron collider experiments, including

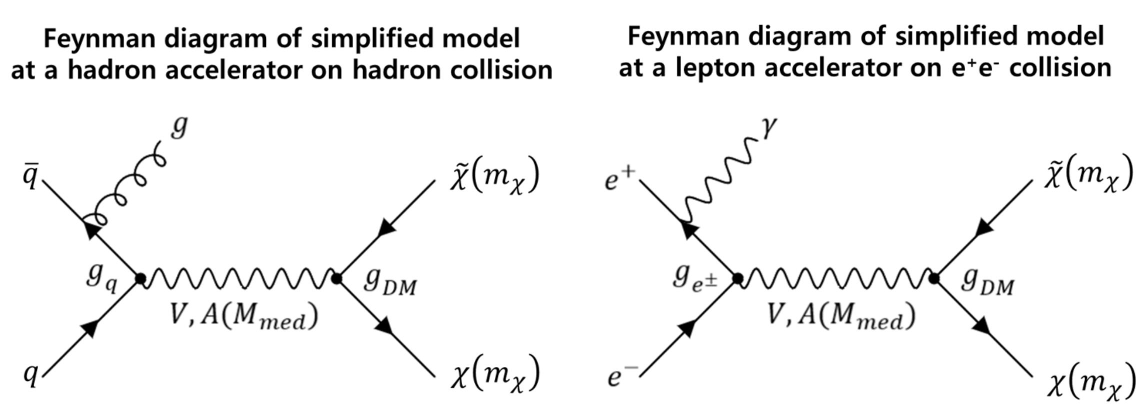

Fig. 1. The comparison of Feynman diagram of the simplified model at hadron and lepton collisions.

Table 1. Parameters of electron-positron accelerators/detectors

Accelerator/detector	Type	$\sqrt{s}$ [GeV]	Circumference or length [km]
CEPC/CEPC	Circular	91 (e^+: 45.5, e^-: 45.5) 160 (e^+: 80, e^-: 80) 240 (e^+: 120, e^-: 120)	100
FCC-ee/IDEA	Circular	91 (e^+: 45.5, e^-: 45.5) 160 (e^+: 80, e^-: 80) 250 (e^+: 125, e^-: 125) 350 (e^+: 175, e^-: 175)	97.75
ILC/ILD	Linear	250 (e^+: 125, e^-: 125)	20.5
		500 (e^+: 250, e^-: 250)	31
		1,000 (e^+: 500, e^-: 500)	40

Adapted from Particle Data Group et al. (2020) with permission of the Oxford University Press.
CEPC, Circular Electron Positron Collider; FCC-ee, Future Circular Collider; IDEA, Innovative Detector for Electron-positron Accelerator; ILC, International Linear Collider; ILD, International Large Detector.

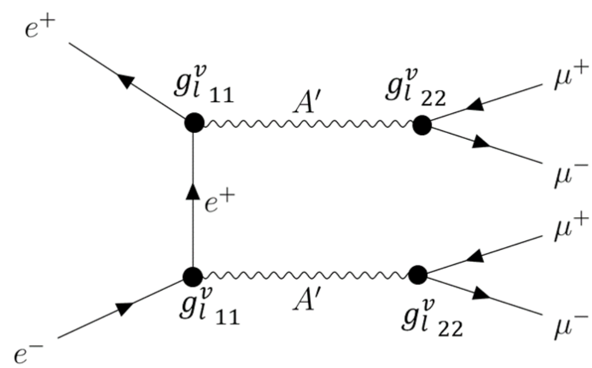

Fig. 2. Dominant Feynman diagrams of double dark photon mode.

Table 2. The summary of coupling constants

Paper	MadGraph5	Value	Description
$g^v_{l\ 11}$	gvl11	0.1	Electron-Y1 vector (A') coupling
$g^v_{l\ 22}$	gvl22	0.1	Muon-Y1 vector (A') coupling

the LHC at European Organization for Nuclear Research (CERN) (Abdallah et al. 2015). However, we modified and utilized this model for electron-positron accelerators. Signal events were generated based on the model using MadGraph5 (Alwall et al. 2014).

3. METHODS

In step 1, we generated events using MadGraph5 (Alwall et al. 2014). In event generation, physical parameters of the $\sqrt{s}$ and dark photon mass had to be scanned, which required a large amount of simulation. Therefore, events were efficiently generated by utilizing the KISTI-5 supercomputer (Park & Cho 2021a, b). In step 2, a detector simulation was performed using Delphes (de Favereau et al. 2014) as the fast simulation. When simulating the detector, Delphes cards (Delphes 2014) were used in each experiment. In step 3, the physical quantities were reconstructed using C++ code and ROOT (Brun & Rademakers 1997). Finally, in step 4, the histogram as a result of reconstruction were fitted with RooFit (Verkerke & Kirkby 2003) to obtain the expected number of signal events.

4. RESULTS

4.1 Center-of-Mass Energy Dependency of Cross-Section

Signal modes include parameters of $\sqrt{s}$ and dark photon mass, which affect cross-section. Therefore, it is necessary to investigate the cross-section according to $\sqrt{s}$ and dark photon mass. In this section, we scanned the cross-section for $\sqrt{s}$. Table 3 lists the specification of the scan for center-of-mass energy. Fig. 3 shows the center-of-mass energy dependency of the cross-section in the decay mode of $e^+e^- \rightarrow A'A'$ (Park et al. 2022). Red vertical lines indicate individual $\sqrt{s}$ of accelerators. Cross-section increases as the $\sqrt{s}$

Table 3. Specification of scan for center-of-mass energy

Specification	Contents
No. of events	10,000
Event generator	MadGraph5 ver. 2.6.6
Model	The Simplified Model
Machine	KISTI-5 supercomputer
Condition	P_{T_μ}, $P_{T_\gamma} \geq 0.01$ GeV
$\sqrt{s}$ [GeV]	[1, 9] in step size of 1 [10, 490] in step size of 10 [500, 3,000] in step size of 100
$m_{A'}$ [GeV]	0.3
Decay width [GeV]	6.7×10^{-6}
$g^v_{l\ 11}$, $g^v_{l\ 22}$	0.1

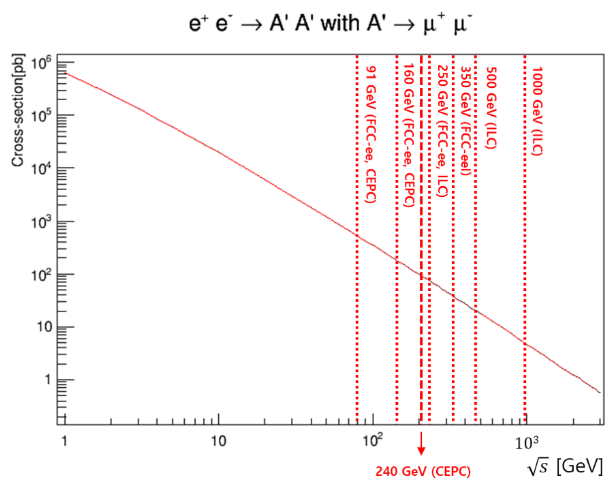

Fig. 3. Center-of-mass energy dependency of the cross-section in the decay mode of $e^+e^- \rightarrow A'A'$ for $m_{A'} = 0.3$ GeV. ILC, International Linear Collider; FCC-ee, Future Circular Collider; CEPC, Circular Electron Positron Collider.

decreases.

4.2 The Dark Photon Mass Dependency of the Cross-Section

The cross-section was scanned for the dark photon mass from 0.25 to 500 GeV. Table 4 lists the specification of the scan for dark photon mass. Fig. 4 shows the dark photon mass dependency of the cross-section in the decay mode of $e^+e^- \rightarrow A'A'$ at each accelerator. As a result, we found dark photon mass with the largest cross-section at each accelerator energy. And then, we applied these dark photon masses to generate signal events for each experiment. Table 5 shows the dark photon masses of $e^+e^- \rightarrow A'A'$ decay mode with the maximum cross-section at each $\sqrt{s}$.

4.3 Generation and Reconstruction for the Given Dark Photon Masses

In the previous section, we found dark photon mass with the maximum cross-section for each accelerator. Using these dark photon masses, we performed generation and reconstruction for specific accelerators/detectors. Table 6 shows the specifications of event generation and reconstruction. The KISTI-5 supercomputer was used for event generation, while a local machine, Scientific Linux OS with 32 cores, was used for detector simulation, reconstruction, and fitting. Detector simulation was performed by applying Delphes cards (Delphes 2014)

Table 4. Specification of scan for dark photon mass

Specification	Contents
No. of events	10,000
Event generator	MadGraph5 ver. 2.6.6
Model	Simplified Model
Machine	KISTI-5 supercomputer
Condition	P_{T_μ} , P_{T_γ} ≥ 0.01 GeV
$\sqrt{s}$ [GeV]	0.02, 3.78, 10.58, 90, 160, 240, 250, 350, 380, 500, 1,000
$m_{A'}$ [GeV]	0.25, 0.5, 0.75, 1.0, 2.5, 5.0, 7.5, 10.0, 25.0, 50.0, 75.0, 100.0, 150, 200, 250, 300, 350, 400, 450, 400, 450, 500
Decay width [GeV]	6.7×10^{-6}
$g^V_{l\,11}$, $g^V_{l\,22}$	0.1

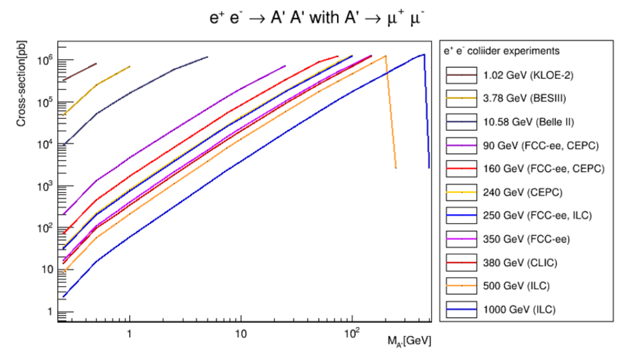

Fig. 4. Dark photon mass dependency of the cross-section in the decay mode of $e^+e \rightarrow A'A'$ at each accelerator. FCC-ee, Future Circular Collider; CEPC, Circular Electron Positron Collider; ILC, International Linear Collider.

Table 5. Dark photon masses ($m_{A'}$) which show the maximum cross-section for each $\sqrt{s}$

Accelerator	$\sqrt{s}$ [GeV]	$m_{A'}$ [GeV]
FCC-ee	91 (e^+: 45.5, e^-: 45.5)	25
	160 (e^+: 80, e^-: 80)	75
	250 (e^+: 125, e^-: 125)	100
	350 (e^+: 175, e^-: 175)	150
CEPC	91 (e^+: 45.5, e^-: 45.5)	25
	160 (e^+: 80, e^-: 80)	75
	240 (e^+: 120, e^-: 120)	100
ILC	250 (e^+: 125, e^-: 125)	100
	500 (e^+: 250, e^-: 250)	200
	1,000 (e^+: 500, e^-: 500)	450

FCC-ee, Future Circular Collider; CEPC, Circular Electron Positron Collider; ILC, International Linear Collider.

Table 6. The specification of event generation and reconstruction

	Specification	Contents
Generation	No. of events	1,000,000
	Event generator	MadGraph5 ver. 2.6.6
	Model	Simplified Model
	Machine	KISTI-5 supercomputer
	Condition	$P_{T,\mu}$, $P_{T,\gamma}$ ≥ 0.01 GeV
	Decay width [GeV]	6.7×10^{-6}
	$g^V_{l\,11}$, $g^V_{l\,22}$	0.1
Reconstruction	Detector simulation	Delphes ver. 3.5.0
	Analysis tool	ROOT ver. 6.24.06
	Machine	Local machine

for each detector. Next, the physical quantities for dark photons were reconstructed using C++ and ROOT (Brun & Rademakers 1997). Finally, the invariant masses of the dark photons were fitted using RooFit (Verkerke & Kirkby 2003). Table 7 lists the reconstruction configuration of each accelerator/detector. Table 8 shows parameters of Delphes for each accelerator/detector. The difference of parameters among Delphes results in difference of detector efficiency (Delphes 2014).

Fig. 5 shows dark photon physical quantities at $\sqrt{s}$ =240 GeV (CEPC/CEPC), $\sqrt{s}$ =350 GeV (FCC-ee/IDEA) and at $\sqrt{s}$ =1,000 GeV (ILC/ILD). Each figure shows physical quantities of the invariant mass of two dark photons ($M_{A'_1A'_2}$), the invariant mass of a dark photon ($M_{A'_1}$), and the transverse momentum of a dark photon ($p_{T\,A'_1}$) in the decay mode of $e^+e^- \rightarrow A'A'$ (Park et al. 2020). To find the muon pair that originates from the associated dark photon, we selected dark photons by choosing the least dark photon mass difference (Park et al. 2021). It reduces the random combinatorial background of $\mu^+\mu^-$. The expected number of events has been obtained by fitting $M_{A'_1A'_2}$ and $M_{A'_1}$, $M_{A'_2}$ with double Gaussian function for both decay mode of $e^+e^- \rightarrow A'A'$.

The results show that the CEPC had the highest detector acceptance among the accelerators. Table 9 summarizes the detector efficiencies of the accelerators/detectors. The difference in the detector efficiencies was attributed to the different Delphes parameters. Fig. 6 shows the detector efficiencies of each accelerator/detector with decay mode of $e^+e^- \rightarrow A'A'$, respectively. These results show sensitivities of the physical potentials of the different electron-positron colliders.

5. SUMMARY

We studied the double dark photon modes of future electron-positron accelerators/detectors. The signal mode was $e^+e^- \rightarrow A'A'$, where A' decaying into a muon pair. We studied sensitivities of double dark photon modes at CEPC/CEPC, FCC-ee/IDEA, and ILC/ILD using the parameterized response of the detector simulation of Delphes. For the generation study, we determined the dark photon mass dependency of the cross-section. We found the dark photon mass at which the cross-section was the highest for each experiment, and these dark photon masses were adapted for reconstruction. In the reconstruction study, we determined the expected number of signal events. Dark photons were selected by selecting the least dark photon mass difference

Table 7. The reconstruction configuration for each accelerator/detector

Accelerator/detector	$\sqrt{s}$ [GeV]	$m_{A'}$ [GeV]	Delphes card (.tcl) (Delphes 2014)
CEPC/CEPC	91 (e^+: 45.5, e^-: 45.5)	25	Delphes_card_CEPC
	160 (e^+: 80, e^-: 80)	75	
	240 (e^+: 120, e^-: 120)	100	
FCC-ee/IDEA	91 (e^+: 45.5, e^-: 45.5)	25	Delphes_card_IDEA
	160 (e^+: 80, e^-: 80)	75	
	250 (e^+: 125, e^-: 125)	100	
	350 (e^+: 175, e^-: 175)	150	
ILC/ILD	250 (e^+: 125, e^-: 125)	100	Delphes_card_ILD
	500 (e^+: 250, e^-: 250)	200	
	1,000 (e^+: 500, e^-: 500)	450	

CEPC, Circular Electron Positron Collider; FCC-ee, Future Circular Collider; IDEA, Innovative Detector for Electron-positron Accelerator; ILC, International Linear Collider; ILD, International Large Detector.

Table 8. Parameters of Delphes for each accelerator/detector

Accelerator/detector	CEPC/CEPC (Delphes 2014)	FCC-ee/IDEA (Delphes 2014)	ILC/ILD (Delphes 2014)
Magnetic field (B)			
Radius [m]	1.81	2.25	1.8
Half-length [m]	2.35	2.5	2.4
B [T]	3.5	2.0	3.5
Muon			
Tracking condition of η	$\lvert\eta\rvert \leq 3.0$	$\lvert\eta\rvert \leq 3.0$	$\lvert\eta\rvert \leq 2.4$
Tracking condition of p_T [GeV]	> 0.1	-	> 0.1
Tracking condition of E [GeV]	-	-	-

CEPC, Circular Electron Positron Collider; FCC-ee, Future Circular Collider; IDEA, Innovative Detector for Electron-positron Accelerator; ILC, International Linear Collider; ILD, International Large Detector.

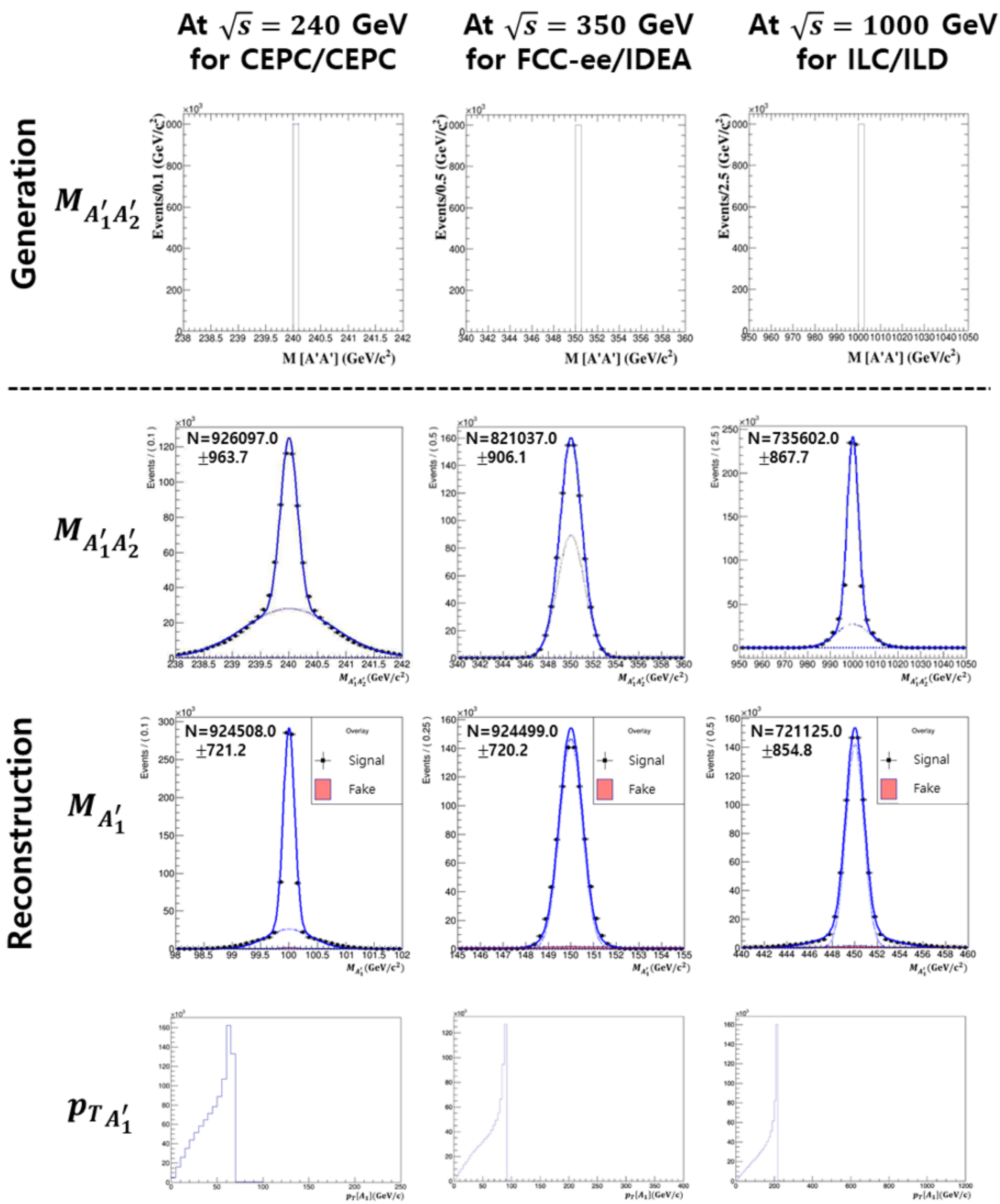

Fig. 5. Dark photon physical quantities at $\sqrt{s} = 240$ GeV (CEPC/CEPC), $\sqrt{s} = 350$ GeV (FCC-ee/IDEA) and $\sqrt{s} = 1,000$ GeV (ILC/ILD). CEPC, Circular Electron Positron Collider; FCC-ee, Future Circular Collider; IDEA, Innovative Detector for Electron-positron Accelerator; ILC, International Linear Collider; ILD, International Large Detector.

to reduce the random combinatorial background. Finally, the detector efficiencies of each accelerator and detector were determined using Delphes. These results show sensitivities of the physical potentials of the different electron-positron colliders. The results can facilitate in identifying double dark photon mode in future electron-positron accelerators and detectors.

Table 9. The summary of detector efficiency for each accelerator

Accelerator/detector	$\sqrt{s}$ [GeV]	$m_{A'}$[GeV]	Detector efficiency [%]
CEPC/CEPC	91 (e^+: 45.5, e^-: 45.5)	25	92.059 ± 0.148
	160 (e^+: 80, e^-: 80)	75	93.595 ± 0.140
	240 (e^+: 120, e^-: 120)	100	93.398 ± 0.161
FCC-ee/IDEA	91 (e^+: 45.5, e^-: 45.5)	25	87.701 ± 0.094
	160 (e^+: 80, e^-: 80)	75	79.259 ± 0.089
	250 (e^+: 125, e^-: 125)	100	83.733 ± 0.092
	350 (e^+: 175, e^-: 175)	150	81.103 ± 0.091
ILC/ILD	250 (e^+: 125, e^-: 125)	100	70.706 ± 0.142
	500 (e^+: 250, e^-: 250)	200	73.560 ± 0.086
	1,000 (e^+: 500, e^-: 500)	450	74.161 ± 0.086

CEPC, Circular Electron Positron Collider; FCC-ee, Future Circular Collider; IDEA, Innovative Detector for Electron-positron Accelerator; ILC, International Linear Collider; ILD, International Large Detector.

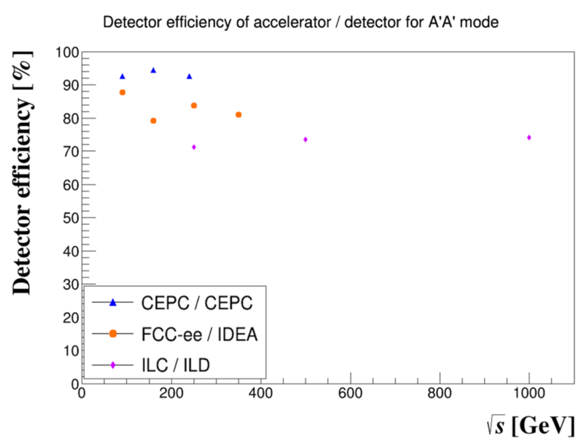

Fig. 6. The detector efficiencies for each accelerator/detector. CEPC, Circular Electron Positron Collider; FCC-ee, Future Circular Collider; IDEA, Innovative Detector for Electron-positron Accelerator; ILC, International Linear Collider; ILD, International Large Detector.

ACKNOWLEDGMENTS

This study was supported by a National Research Foundation of Korea (NRF) grant funded by the Korean government (MSIT) (No. 2021R1F1A1064008). This study was also supported by the major institutional R&D program, KISTI (No. K-23-L02-C04-S01) and National Supercomputing Center with supercomputing resources including technical support (KSC-2023-CHA-0005). A. Sytov acknowledges support by the European Commission through the H2020-MSCA-IF TRILLION project (GA. 101032975).

ORCIDs

Kihong Park https://orcid.org/0000-0003-0567-3493
Kyungho Kim https://orcid.org/0000-0002-4659-1112
Alexei Sytov https://orcid.org/0000-0001-8789-2440
Kihyeon Cho https://orcid.org/0000-0003-1705-7399

REFERENCES

Aaij R, Adeva B, Adinolfi M, Ajaltouni Z, Akar S, et al., Search for dark photons produced in 13 TeV pp collisions, Phys. Rev. Lett. 120, 061801 (2018). https://doi.org/10.1103/PhysRevLett.120.061801

Abdallah J, Araujo H, Arbey A, Ashkenazi A, Belyaev A, et al., Simplified models for dark matter searches at the LHC, Phys. Dark Universe 9-10, 8-23 (2015). https://doi.org/10.1016/j.dark.2015.08.001

Alwall J, Frederix R, Frixione S, Hirschi V, Maltoni O, et al., The automated computation of tree-level and next-to-leading order differential cross sections, and their matching to parton shower simulations, J. High Energy Phys. 07, 79 (2014). https://doi.org/10.1007/JHEP07(2014)079

Brun R, Rademakers F, ROOT: an object oriented data analysis framework, Nucl. Instrum. Methods Phys. Res. Sect. A 389, 81-86 (1997). https://doi.org/10.1016/S0168-9002(97)00048-X

Cho K, e-Science paradigm for astroparticle physics at KISTI, J. Astron. Space Sci. 33, 63-67 (2016). https://doi.org/10.5140/JASS.2016.33.1.63

Cho K, Computational science-based research on dark matter at KISTI, J. Astron. Space Sci. 34, 153-159 (2017). https://doi.org/10.5140/JASS.2017.34.2.153

de Favereau J, Delaere C, Demin P, Giammanco A, Lemaître V, et al., DELPHES 3: a modular framework for fast simulation of a generic collider experiment, J. High Energy Phys. 2, 57 (2014). https://doi.org/10.1007/JHEP02(2014)057

Delphes (2014) Delphes detector cards [Internet], viewed 2022 Oct 28, available from: https://cp3.irmp.ucl.ac.be/projects/delphes/browser/git/cards

He M, He XG, Huang CK, Li G, Search for a heavy dark photon at future e^+e^- colliders, J. High Energy Phys. 3, 139 (2018). https://doi.org/10.1007/JHEP03(2018)139

Hearty C, Searches for dark photons at accelerators, J. Phys. Conf. Ser. 2391, 012011 (2022). https://doi.org/10.1088/1742-6596/2391/1/012011

Ilten P, Soreq Y, Thaler J, Williams M, Xue W, Proposed inclusive dark photon search at LHCb, Phys. Rev. Lett. 116, 251803 (2016). https://doi.org/10.1103/PhysRevLett.116.251803

Morgante E, Simplified dark matter models, Adv. High Energy Phys. 2018, 5012043 (2018). https://doi.org/10.1155/2018/5012043

Park J, Chang J, Cheung K, Lee JS, Measuring the trilinear Higgs boson self-coupling at the 100 TeV hadron collider via multivariate analysis, Phys. Rev. D 102, 073002 (2020). https://doi.org/10.1103/PhysRevD.102.073002

Park K, Cho K, A study of dark photon at the electron-positron collider experiments using KISTI-5 supercomputer, J. Astron. Space Sci. 38, 55-63 (2021a). https://doi.org/10.5140/JASS.2021.38.1.55

Park K, Cho K, Study of dark matter at e^+e^- collider using KISTI-5 supercomputer, Int. J. Contents. 17, 67-73 (2021b). https://doi.org/10.5392/IJoC.2021.17.3.067

Park K, Kim K, Cho K, A study of double dark photons produced by lepton colliders using high performance computing, J. Astron. Space Sci. 39, 1-10 (2022). https://doi.org/10.5140/JASS.2022.39.1.1

Park SH, Kwon YJ, Adachi I, Aihara H, Al Said S, et al., Search for the dark photon in $B^0 \to A'A'$, $A' \to e^+e^-$, $\mu^+\mu^-$, and $\pi^+\pi^-$ decays at Belle, J. High Energy Phys. 4, 191 (2021). https://doi.org/10.1007/JHEP04(2021)191

Particle Data Group, Zyla PA, Barnett RM, Beringer J, Dahl O, et al., Review of particle physics, Prog. Theor. Exp. Phys. 2020, 083C01 (2020). https://doi.org/10.1093/ptep/ptaa104

San YC, Perelstein M, Tanedo P, Dark Z at the international linear collider, Phys. Rev. D 106, 015027 (2022). https://doi.org/10.1103/PhysRevD.106.015027

Shuve B, Yavin I, Dark matter progenitor: light vector boson decay into sterile neutrinos, Phys. Rev. D 89, 113004 (2014). https://doi.org/10.1103/PhysRevD.89.113004

Verkerke W, Kirkby D, The RooFit toolkit for data modeling, Proceedings of the Talk from the 2003 Computing in High Energy and Nuclear Physics, La Jolla, CA, USA, 24-28 Mar 2003.

Yeo I, Cho K, Researches on dark matter using $e^+ e^-$ collider, J. Astron. Space Sci. 35, 67-74 (2018). https://doi.org/10.5140/JASS.2018.35.2.67